Applied Petrochemical Research (2020) 10:1–12
https://doi.org/10.1007/s13203-019-00239-2

ORIGINAL ARTICLE

Adsorptive desulfurization of diesel using activated sewage sludge: kinetics, equilibrium and thermodynamics studies

David Stan Aribike[1] · **Mohammed Awwalu Usman**[1] · **Mojirade M. Oloruntoba**[1]

Received: 3 May 2019 / Accepted: 13 November 2019 / Published online: 7 December 2019
© The Author(s) 2019

Abstract

Combustion of fossil fuels gives rise to sulfur oxides, which are harmful to the environment. Adsorptive desulfurization (ADS) of diesel was conducted using sewage sludge activated with H_2O_2 as the oxidizing agent. A full 2^2 central composite response surface design was employed to determine optimum conditions for the production of activated sewage sludge (ASS). The adsorbent (ASS) was characterized using SEM, EDX and FTIR and the results of the analysis showed that it has the capacity to desulfurize diesel significantly. The ASS was subsequently used to conduct batch ADS of diesel with a view to investigate the kinetics, equilibrium and thermodynamics of the process. The optimum conditions established for the production of ASS using H_2O_2 as the oxidizing agent were: temperature 400 °C and holding time 60 min. The Elovich model gave the best fit to the kinetic data of the ADS of diesel using ASS, while the equilibrium study showed that the Freundlich isotherm fitted the data at 35 °C better than Temkin and Langmuir isotherms. The positive values of the free energy and enthalpy changes revealed that the process was non-spontaneous and endothermic, respectively, while the negative entropy change is evidence of decrease in randomness of the adsorbed species. 33% desulfurization was achieved in 100 min during ADS of diesel showing that the adsorbent developed by activating SS with H_2O_2 was very good and effective. Thus, ASS can be used to gain more insight into kinetics, equilibrium and thermodynamics of the ADS of middle-distillate petroleum fractions.

Keywords Adsorptive desulfurization · Sewage sludge · Kinetics · Thermodynamics · Isotherm · Diesel

Introduction

Fossil fuels are any carbon-containing fuels derived from the decomposed remains of prehistoric plants and animals, e.g., petroleum, coal, peat and natural gas. The problem with these fossil fuels is that when combusted they give rise to emissions (CO_x, SOx, NOx, VOCs) that are harmful to the environment. Carbon dioxide emissions are known to be major contributor to global warming (climate change). Sulfur and nitrogen oxides emissions are pollutants which have been shown to be responsible for acid rain, which destroys the environment and infrastructures [7].

Governments throughout the world have recognized the problems associated with these emissions and have taken steps to reduce them through legislations. Environmental agencies are also imposing more stringent regulatory standards on the sulfur content of petroleum products such as gasoline and diesel oil. Organic sulfur compounds, namely, thiols, sulfides, and thiophenes in lower-boiling fractions of petroleum distillate, such as the gasoline range, are readily removed by conventional chemical hydro-desulfurization (HDS) method used in refineries. Furthermore, middle-distillate fractions, such as the diesel and fuel oil range, contain significant amounts of benzothiophene (BT) and dibenzothiophene (DBT), which are recalcitrant and comparatively more difficult to remove by HDS. Due to their resistance to HDS, these compounds represent a significant barrier to reaching very low sulfur levels in middle and heavy-distillate range fuels [9]. Current trends toward stricter regulations on the content of sulfur in fuels provide enough incentive for the continued search for desulfurization techniques. Adsorptive desulfurization is amongst the techniques that can be explored.

Adsorptive desulfurization (ADS) is a process that depends on the ability of an adsorbent to selectively adsorb

✉ David Stan Aribike
dupearibike@yahoo.co.uk

[1] Department of Chemical and Petroleum Engineering, University of Lagos, Lagos, Nigeria

organosulfur compounds onto tailored surfaces which are employed as adsorbents. ADS utilizes adsorbent materials known to be multifunctional in terms of structural, textural and surface properties to match the requirement for the adsorption of sulfur containing compounds, thereby yielding clean fuel under modest process conditions. A number of studies have been reported in the literature on ADS.

Xiaoliang et al. [21] studied two model diesel fuels (MD-1 and MD-2) with different concentrations of DBT over Adsorbent-6, which was prepared from CoMo oxides supported on γ-alumina (CoMo/γ-Al_2O_3; CoO: 3 wt%; MoO_3: 14 wt%; Surface area: 183 m^2/g; Pore volume: 0.4755 ml/g; Average pore size: 102 Å). MD-1 contains the same molar concentration of DBT, 4-methyldibenzothiophene (4-MDBT), dimethyl dibenzothiophene (4,6-DMDBT), and 1 methylnaphalene (1-MNA), while MD-2 contains only one sulfur compound, DBT; and the total sulfur concentration in MD-1 and MD-2 was 486 ppm and 200 ppm, respectively. The adsorptive desulfurization of MD-1 over Adsorbent-6 at 50 °C was studied, and it was found that the adsorption selectivity increased in the order of DBT > 4-MDBT > 4,6-DMDBT. Also, the ADS of MD-2 over Adsorbent-6 at 50 °C and 150 °C was conducted, and it was found that the performance was poorer at 150 °C than at 50 °C indicating that lower temperature was better for the ADS over this type of adsorbents. Selvavathi et al. [15] developed process for the desulfurization of diesel, with an initial sulfur content of 737 ppm. Removal of sulfur compounds, refractory compounds in particular, was achieved under room temperature and atmospheric pressure in sharp contrast to the conventional HDS process wherein the operation conditions are severe. In addition to the removal of appreciable amounts of sulfur from the diesel feed, the carbon materials employed for ADS were found to be completely regenerable. Khodadadi et al. [8] showed that copper oxide (CuO) nanoparticles could be used as adsorbent for the desulfurization of liquid fuels. The result showed that temperature had an effect on removal of total sulfur and that the sorption rate of sulfur removal was independent of whether the sample was agitated or not. The kinetic study for this adsorption process showed that the reaction path was second order. Thitiwan et al. [20] investigated the removal of DBT from n-octane using an adsorption process with sewage sludge-derived activated carbons (S-ACs) at ambient conditions. The effect of varying the type of activating agent ($ZnCl_2$, HNO_3 and KOH), activating agent/char weight ratio (0.5–6 w/w), carbonization temperature (400–800 °C) and time (0.5–2 h) on the physicochemical properties and the adsorptive capacity of the S-ACs was investigated. All the studied parameters were found to play an important role on the physicochemical properties as well as the surface chemistry of the S-ACs. The DBT adsorptive capacity increased as the oxygen-containing functional groups increased, especially the carbonyl group. The S-AC prepared by KOH-activation exhibited the highest adsorptive capacity with up to 14.12 mg/g or around 70.6% DBT removal, which was greater than that of a commercial activated carbon (C-AC). The adsorption of DBT via S-AC followed the Langmuir isotherm. Nada et al. [11] studied the desulfurization of a simulated diesel fuel at ambient temperature and pressure by different adsorbents in three different adsorption beds containing commercial activated carbon (AC); Cu-Y zeolite; and layered bed of 15 wt% AC, followed by Cu-Y zeolite. The adsorbents tested for total sulfur adsorptive capacity followed the order AC/Cu-Y zeolite > Cu-Y zeolite > AC. Ahmad et al. [1] studied selective ADS of kerosene and diesel oil by incorporating different metals which included Fe, Cr, Ni, Co, Mn, Pb, Zn and Ag on montmorollonite clay (MMT) by wet impregnation method. In the procedure, stoichiometric amounts of 0.2 M solution of different metals precursors, i.e., $Fe(NO_3)_3$, $Cr(NO_3)_2$, $Ni(NO_3)_2$, $Co(NO_3)_2$, $MnCl_2$, $Pb(NO_3)_2$, $ZnCl_2$ and $Ag(NO_3)_2$ were mixed with 3 g of the surface area, and the pore size and pore volume of the MMT were found to increase many fold with Zn impregnation. Rashidi et al. [13] studied the performance of aluminosilicate meso structure (MSU-S) and its modified forms with phosphotungstic acid (HPW) and nickel oxide-HPW (NiO-HPW) for the desulfurization and denitrogenation of model diesel fuels. The results of the characterization showed that MSU-S modified with HPW causes higher acidity along with a negligible loss in structural aspects, while the MSU-S modified with NiO-HPW leaves a negative effect on the mesoporous structure, crystalline phase, and particle shape along with a high positive impact on surface acidity. Both modified adsorbents perform selectively toward nitrogen removal over sulfur compounds. The pseudo-second-order model best fitted the kinetics data and Freundlich model best explained the equilibrium isotherm for all species over NiO/HPW-MSU-S. Saleh and Danmaliki [14] investigated the utilization of waste rubber tyres as a low cost adsorbent for ADS of DBT from fuels. The rubber tyres were converted into activated carbon by pyrolysis, activation and chemical treatment with 4 M HNO_3 for 3 h at 90 °C to enhance the surface functionalities. The treated rubber tyres yielded carbon with enhanced surface functionalities. Moreira et al. [10] studied the desulfurization of real and synthetic naphthenic oil (obtained by adding thiophene (T), BT and DBT in a wide range of concentrations to a matrix comprised of decahydronaphthalene (DHN)), respectively, using an adsorbent (obtained from coconut shell) at different temperatures. It was found that water, carbazole, naphthalene and phenol in the synthetic naphthenic oil have strong inhibiting effects on the desulfurization performance of the adsorbent

at 100 °C and that increasing the temperature to 150 °C significantly improved the performance of the adsorbent in the desulfurization of real naphthenic oil. The results also showed that the adsorbent exhibited a remarkable adsorption performance as the adsorption capacities reached 1.6×10^5, 2.0×10^5 and 1.9×10^5 mg/g for T, BT and DBT in DHN, respectively. Sikarwar et al. [17] explored the use of cobalt-modified, acetic-acid treated granular activated carbon (GAC) adsorbent for ADS of DBT-containing model oil. The modification and treatment of the GAC improved its adsorption capacity and 92% of DBT removal was achieved under optimized operating conditions. It was found that the Redlich Peterson model best fitted the experimental data over Langmuir, Freundlich and Temkin models. The changes in entropy and heat of adsorption were estimated to be 0.177 kJ/(mol K) and 35.67 kJ/mol, respectively. It was concluded that cobalt-incorporated, acetic-acid-activated GAC proves to be a potential adsorbent for the removal DBT from fuel in an economic and environmental friendly way. Shah et al. [16] explored the selective desulfurization of model oil and the commercial kerosene and diesel using 37% concentrated HCl acid-modified activated charcoal (AC) as an adsorbent. The adsorption capacity of the AC was evaluated for the removal of DBT present in the fuel under certain experimental conditions. The results showed that the adsorption followed pseudo-second-order kinetic model and the experimental data fitted both the Langmuir and Freundlich adsorption isotherm models.

Most of the previous works used model fuel rather than real fuel. Furthermore, there is limited information on the kinetics and thermodynamics of ADS. Hence, the aim of this work is to study the adsorptive desulfurization of Nigeria diesel using sewage sludge activated with H_2O_2. The kinetics, equilibrium and thermodynamics studies were also carried out.

Materials and methods

Materials

The diesel fuel was purchased locally from the Nigerian National Petroleum Corporation (NNPC) filling station at Rainbow bus-stop along Oshodi-Mile 2 Expressway, Lagos, Nigeria. The H_2O_2 and HCl used were of analytical grade. The sewage sludge collection area was at Service Area of University of Lagos, Lagos Nigeria, located in the South Western part of Nigeria on geographical coordinates of 6° 27′ 11″ N, 3° 23′ 45″ E. The SS samples were collected in a plastic container through the 150 mm sewer pipe channel from the Septic tank to the constructed wetland during a dislodgement process of the tank and taken immediately to the laboratory for treatment.

Methods

The main physicochemical properties of the diesel fuel were analyzed using different American Society for Testing and Materials [2] standard methods and the results noted. The methods employed involved the pretreatment, activation and characterization of the sewage sludge, batch adsorptive desulfurization of diesel and the kinetics, equilibrium and thermodynamics studies as presented in the sections below.

Pretreatment and activation of sewage sludge

The SS sample collected was filtered by a simple filtration process to dewater the sludge. The dewatered sludge was dried in open air for 7 days before transferring to an oven set at 105 °C and removed when a constant weight was noted. To have homogeneity, the sample was crushed into semi-fine powder and sieved to size range of 37–149 μm which corresponds to the size of commercial activated carbon.

The activated sewage sludge (ASS) was prepared by impregnating measured samples of treated SS with H_2O_2. Each of the impregnated sewage sludge samples was then stirred and left for about 3 h. The mixtures obtained for each of the samples were oven dried at a temperature of 110 °C until a constant weight was observed. To attain maximum surface area and porosity of sample, carbonization of the impregnated sample was carried out in a Gallenkamp Muffle furnace (Model SXH-1008) with internal dimensions of $38\times25\times14$ cm at a constant input power of 4 kW and a frequency of 50 Hz. About 300 g of the impregnated sample was placed in the muffle furnace and held for 1–2 h at an average heating rate of 10 °C/min at various carbonization temperatures ranging from 400 to 950 °C. The variation of temperature and time was for the purpose of optimizing the process conditions. Each of the different, cooled and carbonized samples was subjected to 0.1 N HCl rinsing (as rinsing with acid removes the majority of acid-soluble inorganic matter and impurities found in the sludge) followed by rinsing with distilled water several times until the pH of washing effluent reached 6–7. The distilled water removed any quantity of HCl that may still be present in the material. The washed sample was then filtered with 0.45 μm filter before drying to a constant weight in an oven at a temperature of 110 °C. When cooled, the samples were sieved to a uniform granular size of 37–149 μm and stored in vacuum desiccators for characterization.

Table 1 Levels of factors in response surface design

Factors	Variables	Low level (− 1)	High level (+ 1)
Temperature (°C)	T	400	950
Time (min)	t	60	120

Table 2 2^2 Response surface design

Experimental run	Block	Coded time t	Coded temperature T	Uncoded time t (min)	Uncoded temperature T (°C)
1	1	− 1	− 1	60	400
2	1	1	− 1	120	400
3	1	− 1	1	60	950
4	1	1	1	120	950
5	1	− 1.4	0	48	675
6	1	1.4	0	132	675
7	1	0	− 1.4	90	286
8	1	0	1.4	90	1064
9	1	0	0	90	675

Optimum conditions for activation of SS

The percentage of sulfur removal (y) depends on factors such as the activating temperature (T) and the holding time (t) during the carbonization process. The modeling of the ADS study was carried out using a full 2^2 RSM with central composite design. The two process factors were simultaneously varied in the experiment using CCD and the two levels were coded as − 1 (low) and + 1 (high) [3]. Table 1 shows the levels defined for the 2^2 response surface design.

To determine the optimum conditions of the activation of SS, experiments were carried out at varying conditions. The experiment was carried out with Minitab 18 (trial version) using a full 2^2 RSM with central composite design. In addition to the four (4) factorial points (which fall within the levels of the different factors) used in the design, one (1) center point and four (4) axial points (which fall outside the levels of the different factors) were also generated by the design. Table 2 shows the code and non-coded experimental design at varying conditions.

Characterization of activated sewage sludge (ASS)

To characterize the ASS, samples were subjected to scanning electron microscopy (SEM), energy dispersive X-rays (EDX) and Fourier transform infrared spectroscopy (FTIR) analyses.

The morphology of the respective ASS used before and after the adsorption study was examined by mounting the samples on sample stubs and automatically analyzed using Field Emission Scanning Electron Microscope (JSM-7600F) with an accelerating voltage of 20 kV and working distance of 8–9 mm. The compositions of the ASS samples used before and after the adsorption study at different magnifications were examined by Oxford Instrument X-Max X-Ray Spectrometer, incorporated with INCA software for elemental analyses. Table Top Bruker FTIR spectrometer (Alpha, Laser Class 1, Platinum ATR model) was used to identify the functional groups present in the SS, ASS (before adsorption) and ASS (after adsorption). The spectra of the samples were recorded in a wave number range of 4000–400 cm^{-1}.

Batch adsorptive desulfurization of diesel

Different masses of adsorbents (3, 6, 9, 12, 15 and 18 g) were used at different temperatures (25, 30, 35, 40, 45 and 50 °C) and varying time of interval of 15 min to reveal the effect of those parameters on the percentage sulfur removal. In a typical run, a specified mass of adsorbent was added to 50 ml of diesel in a conical flask set at a specified temperature and agitated at a speed of 120 rpm over a time of 100 min, respectively. The quantitative analysis of sulfur content in the untreated diesel sample and the desulfurized diesel sample was determined using Shimadzu Multi-type Inductively Coupled Plasma Atomic Emission Spectroscopy (ICP-AES), (ICPE-9000) with a maximum frequency output of 1.6 kW; wavelength range of 167–800 nm and equipped with ICPE solution Software. For each of the samples, a duplicate was analyzed to track experimental error.

Kinetics study

The data obtained at different times before attainment of equilibrium (at 120 min) depict the kinetics.

These data were analyzed using four kinetic models; the pseudo-first-order (PFO), the pseudo-second-order (PSO), Elovich model and the intra-particle diffusion model. For the PFO model, the value of $\log\left(q_e\right)$ was estimated as the intercept of the plot of $\log\left(q_e - q_t\right)$ against t, while k_1 was estimated from the slope of the plot; for the PSO, the plot of $\frac{t}{q_t}$ against t gave the slope as $\frac{1}{q_e}$ from where q_e was estimated. Consequently, the value of k_2 was obtained from the intercept of the plot; while for the Elovich model, the plot of q_t vs. ln t gave a straight line with a slope of $(1/\beta)$ and intercept of $1/\beta$ ln $(\alpha\ \beta)$. The intercept of the intra-particle diffusion plot reflects the boundary layer effect. The q_t versus $t^{1/2}$ plot was linear and did not pass through the origin.

Equilibrium study

The experimental results obtained at a time of 120 min were analyzed using the Langmuir, Freundlich and Temkin

isotherm models for the ADS at 25, 30, 35, 40, 45 and 50 °C, respectively. The analyses were carried out using the linear forms of the isotherms. For the Langmuir isotherm, the plot of $\frac{C_e}{q_e}$ against C_e gave a slope of $\frac{1}{q_m}$ from where q_m was estimated and the value of K_L obtained from the intercept of the plot. For the Freundlich isotherm, the plot of $\ln\left(q_e\right)$ against $\ln\left(C_e\right)$ gave an intercept of and a slope of $\frac{1}{n}$ from where n and K_F were estimated; while for the Temkin isotherm, the plot of q_e against $\ln C_e$ gave B as the slope. Consequently, the value of A was obtained from the intercept of the plot.

Thermodynamics study

The equilibrium data obtained at the following temperatures 25, 30, 35, 40, 45 and 50 °C were analyzed to obtain thermodynamic parameters. A plot of $\ln K_c$ against $1/T$ using Eyring equation gave a straight line with slope $(-\Delta H^0/R)$ and intercept $(\Delta S^0/R)$, from where ΔH^0 and ΔS^0 were evaluated. The change in Gibb's free energy (ΔG^o) was also determined.

Results and discussion

Physicochemical properties of diesel fuel

The main physicochemical properties of the diesel fuel analyzed are shown in Table 3, with a sulfur content of 1390 ppm. This sulfur content is far in excess of the allowable limit of 10–15 ppm (Europe, USA and Japan) and hence the need for desulfurization of the diesel. Though Nigeria crude oil is sweet, diesel in the market still contains a significant amount of sulfur (Refineries and Petrochemicals, NNPC). Thus, in line with the Nigerian government's commitment to reduce emission to protect human health, the Federal Ministry of Environment in collaboration with Standard Organization of Nigeria (SON) after due consultations with relevant stakeholders, successfully reviewed the specified level of sulfur acceptable in diesel (as from July 1, 2017) to a maximum level of 50 ppm (NIS 948:2017) as against the old edition of NIS 149: 2006 Standard for gas oil (diesel oil) which was 3000 ppm [22, 23].

Optimization condition for the sewage sludge

The importance and interactions of the factors, namely temperature and time were evaluated with a 2^2 full RSD using Minitab 15 statistical software (trial version). The response variable in this study is the percentage sulfur removal, y. Table 4 shows the estimated regression coefficients for y. The positive signs in the model coefficients refered to synergetic effects while the negative sign was an indication of antagonistic effect.

The significance of the regression coefficients was determined by applying a Student's t test. The analysis of variance (ANOVA) was used in estimating the main effects and the interaction effects. The effects which have P values less than 0.05 were considered potentially significant while the statistically insignificant factors were discarded. Observation from the design showed that the coefficient of determination, $R^2 = 0.96$; both factors have significant effect on y, the quadratic terms were insignificant and there was no significant interaction between the two factors. The response surface design with results is shown in Table 5.

The predicted percentage sulfur removal $\bar{y}$ is given by

$$\bar{y}\,(\text{Predicted}) = 18.5612 + 1.9544T + 4.5170t - 0.4631T^2 + 0.9757t^2 + 2.6079Tt \quad (1)$$

Table 4 Estimated regression coefficients for the model equation

Term	Coefficient	SE coefficient	S	P
Constant	18.5612	1.7288	10.736	0.002
T	1.9544	0.6112	3.197	0.049
t	4.5170	0.6112	7.390	0.005
$T*T$	−0.4631	1.0136	−0.457	0.679
$t*t$	0.9757	1.0136	0.963	0.407
$T*t$	2.6079	0.8644	3.017	0.057

Table 3 Physico-chemical properties of diesel fuel

S/N	Parameter	ASTM method	Results
1	Specific gravity @ 27 °C	ASTM D1298	0.862
2	Color	ASTM D1500	3
3	Flash point (Pensky Martens open cup)	ASTM D93	62
4	Kinematic viscosity @ 27 °C	ASTM D445	5.1
5	Cloud point °C	ASTMD2500	3
6	Water content by distillation	ASTM D95	Not detected
7	Diesel index	ASTM D611	49
8	API gravity	ASTM D287	32.65
9	Sulfur content (ppm)	ASTM D5453	1390

Table 5 2^2 Response surface design

Experimental run	Coded time t	Coded temp T	Uncoded time t (min)	Uncoded temp T (°C)	y (predicted) (%)	y (experimental) (%)	Residual (%)
1	−1	−1	60	400	15.21	14.39	−0.82
2	1	−1	120	400	13.90	15.11	1.21
3	−1	1	60	950	19.03	17.63	−1.40
4	1	1	120	950	28.15	28.78	0.62
5	−1.4	0	48	675	14.87	16.40	1.53
6	1.4	0	132	675	20.40	19.06	−1.33
7	0	−1.4	90	286	14.13	13.81	−0.31
8	0	1.4	90	1064	26.90	27.41	0.51
9	0	0	90	675	18.56	18.56	0.00

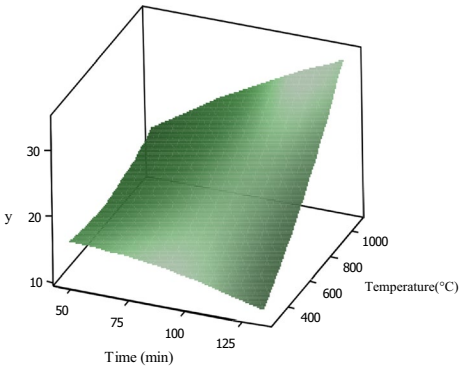

Fig. 1 Surface plot of interactive effect of T and t on y

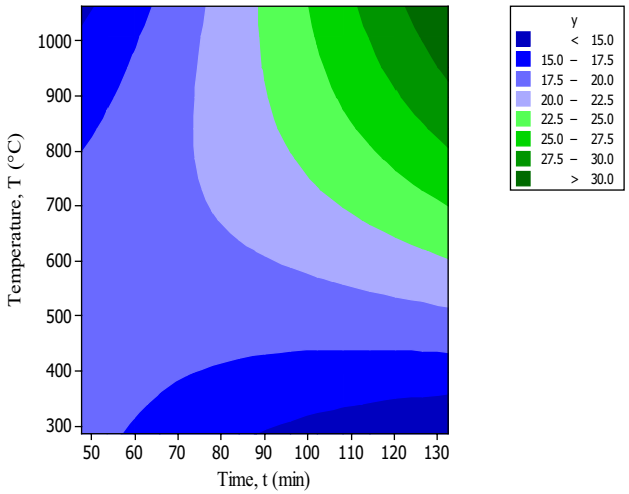

Fig. 2 Contour plot of y vs T and t

The resulting optimum factors obtained from Eq. (1) are $T = -1$ and $t = -1$ which on substitution gives $\bar{y}$ (Predicted) = 15.21%. This corresponds to the predicted value obtained in Table 4. Also, the residual (which is the difference between the y (Experimental) and $\bar{y}$ (Predicted)) was −0.822 and the standard error of prediction was 1.367. Observation from the design showed that an optimum value of $y = 14.39\%$ was obtained using a temperature of 400 °C and holding time of 60 min. The ASS was, therefore, prepared at these conditions. The effects of temperature and holding time were found to be significant but there was no interaction between them.

Response surface and contour plots

To determine the optimum values for the design, response surface and contour graphs were plotted to investigate the interaction among the factors namely, temperature (T) and time (t) with y as shown in Figs. 1 and 2 respectively. Other plots were also generated for the design. The population normality was checked with a normal probability plot of residuals as shown in Fig. 3. If the model was adequate, the plot should resemble a straight line. A check on the

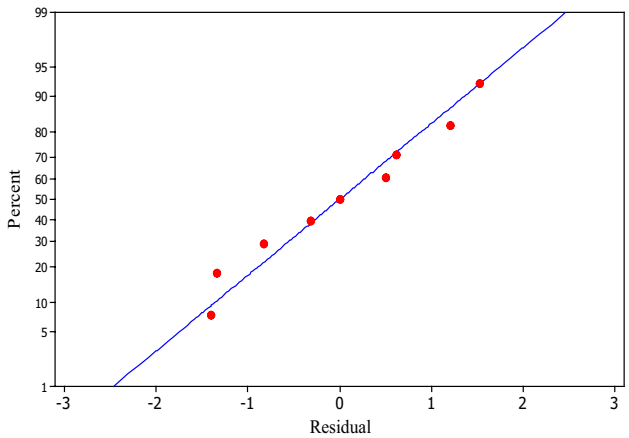

Fig. 3 Normal probability plot of residuals

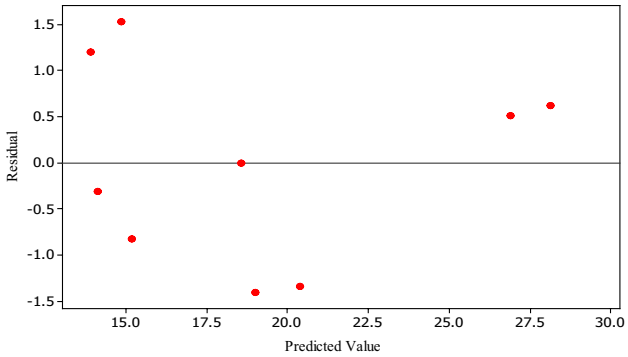

Fig. 4 Plot of residual versus predicted values

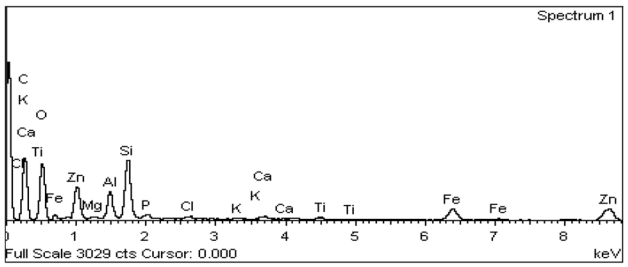

Fig. 5 EDX spectrum for SS (before desulfurization)

plot showed that majority of the residuals fall on a straight line. This implied that the errors were distributed normally. Figure 4 showed the plot of residuals versus fitted values. The plot showed that all experimental data points were uniformly distributed around the mean of the response variable which implied that the model proposed was adequate. The adequacy of the model in Figs. 4 and 5, respectively, was investigated by examining the residuals as described by Cheng et al. [4].

Characterization

The textural characterization of the MSS showed a specific surface area = 70.15 m^2/g; pore diameter = 6.45 nm and pore size distribution = 11.95.

The SEM analysis showed the micrographs of the relative sizes of the samples at different magnifications. These micrographs clearly revealed the difference in the surface morphology of the SS and ASS before and after desulfurization. The micrographs at × 100 magnification and wavelength of 100 µm before and after desulfurization for SS and ASS are shown in Fig.6 a–d. Comparison of Fig. 6a, b showed an increase in formation of pores, indicating the presence of more pores after the SS was activated. Also a comparison of Fig. 6b, d showed that the pores present

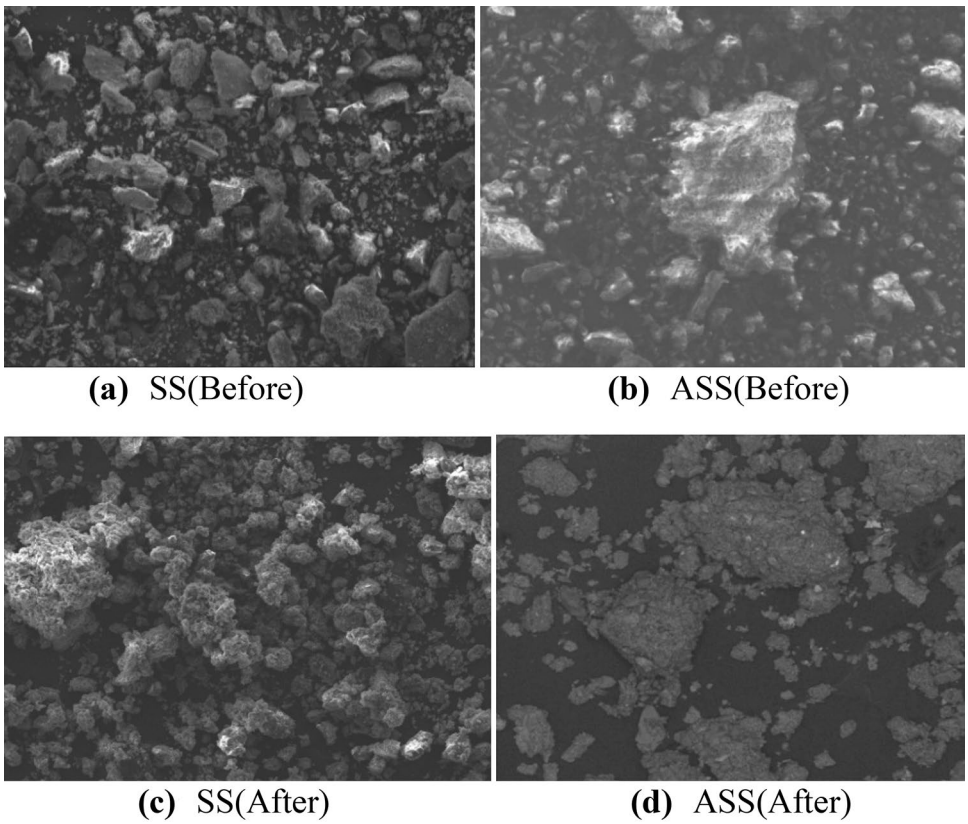

Fig. 6 Micrographs for SS and ASS. **a** SS (before), **b** ASS (before), **c** SS (after), **d** ASS (after)

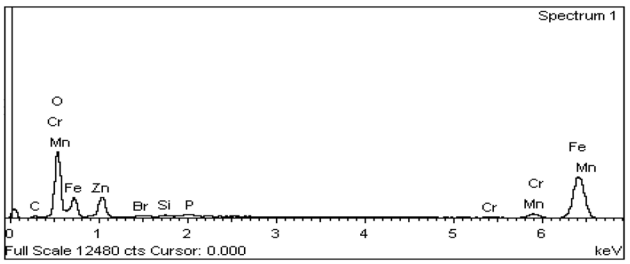

Fig. 7 EDX spectrum for ASS (before desulfurization)

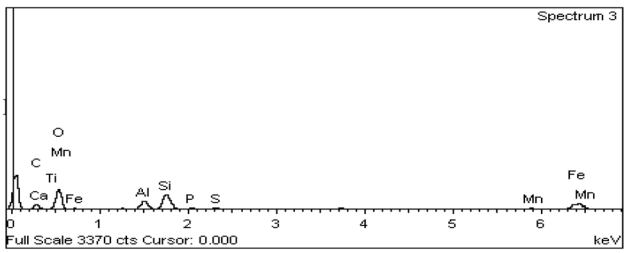

Fig. 8 EDX spectrum for SS (after desulfurization)

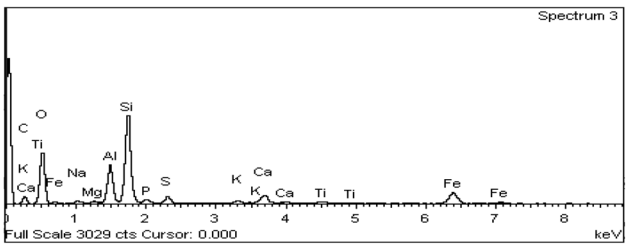

Fig. 9 EDX spectrum for ASS (after desulfurization)

before the desulfurization experiment had been occupied by the adsorbate.

The EDX showed the spectra depicting the peaks of the various elements present and their percentages contained in the samples. It was observed that the SS treated with H_2O_2 had the ability to desulfurize diesel. The spectra at 600 µm before desulfurization experiment for SS and ASS are shown in Figs. 5 and 7, respectively, while those after desulfurization experiment for SS and ASS are shown in Figs. 8, 9.

The spectra in Fig. 9 provided a significant evidence of sulfur adsorption unto the ASS, whereas there was a little trace of sulfur in the SS after desulfurization (Fig. 8) indicating the suitability of the activated sewage sludge to adsorb sulfur.

To understand the types of functional groups present in the samples, FTIR spectrum of the ASS (before adsorption) and ASS (after adsorption) was taken and displayed in Figs. 10 and 11. The ASS (before adsorption) of the adsorbents showed peaks with varying intensities centered around 593–3412 cm^{-1} as shown in Fig. 10. The peaks that appeared at 3406–3412 cm^{-1} were attributed to the strong and broad C–O stretch of alcohol and N–H stretch of amines. The peaks centered at 1622 cm^{-1} and 1621 cm^{-1} were attributed to weak C=C stretch of alkenes and strong N–H stretch of amines. The peaks at 1020 cm^{-1} and 1026 cm^{-1} were attributed to weak C–N stretch of amines: very strong C–F stretch of alkyl halides and C–O stretch of esters. Peaks at 776–794 cm^{-1} were attributed to strong C–H bend and out-of-plane ring bends of aromatic compounds. The peaks centered at 669 cm^{-1} were attributed to strong broad C–H bend of alkynes. The last peaks that appeared at 593 cm^{-1} and 594 cm^{-1} were attributed to strong C–Br stretch of alkyl halides.

In addition to the peaks displayed by this sample, the peaks for the ASS (after adsorption) were also studied as shown in Fig. 11. The peak centered at 3383 cm^{-1} was attributed to C–H stretch of alkynes.

The peaks between 2853 and 2954 cm^{-1} were attributed to strong C–H stretch of alkanes and strong broad O–H stretch of carboxylic acids. The peak centered at 1621 cm^{-1} was attributed to weak C=C stretch of alkenes and strong N–H stretch of amines; the peak centered at 1460 cm^{-1} was attributed to medium strong ring C=C stretch of aromatic compounds and the peak at 1377 cm^{-1} was attributed to medium CH_3C–H bend of alkanes and alkyls. The peak at 1013 cm^{-1} was attributed to weak C–N stretch of amines:

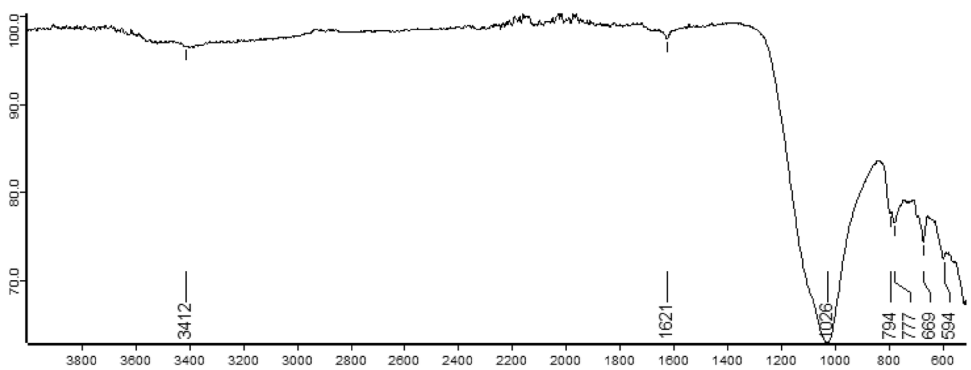

Fig. 10 FTIR spectrum for ASS (before desulfurization)

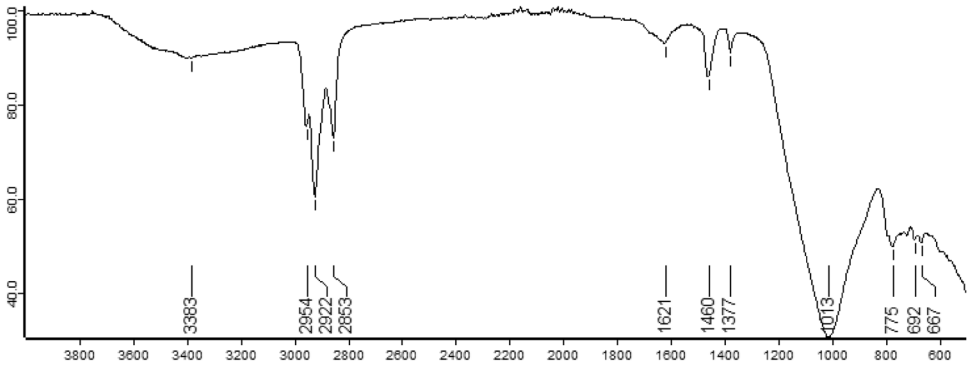

Fig. 11 FTIR spectrum for ASS (after desulfurization)

very strong C–F stretch of alkyl halides and C–O stretch of esters. The peak at 775 cm^{-1} was attributed to strong C–H bend and out-of-plane ring bends of aromatic compounds. The peak centered at 692 cm^{-1} was attributed to strong broad C–H bend of alkynes, while the last peak at 667 cm^{-1} was attributed to strong broad C–H bend of alkynes and strong C–Br stretch of alkyl halide. The peaks for this sample showed higher intensities for all stretches ranging from the alkanes, alkenes, alkynes and other aromatic compounds which could well explain that the adsorption of diesel by the sample.

Adsorptive desulfurization of diesel

Kinetic study

The summary of the best fitted plots for the four (4) different kinetic models at different temperatures is shown in Table 6.

The best fitted Lagergren's pseudo-first-order (PFO) occurred at 30 °C, with a rate constant, $k_1 = 4.96 \times 10^{-2}$ g/mg/min ($R^2 = 0.98$), while the best fitted pseudo-second-order (PSO) occurred at 45 °C with the kinetics rate constant, $k_2 = 2.81 \times 10^{-3}$ g/mg/min ($R^2 = 0.95$). The Elovich model was also used to obtain the initial adsorption rate, α and the desorption constant, β at the different temperatures. The best fitted for the model was obtained at 50 °C ($R^2 = 0.98$); $\alpha = 1.03 \times 10^{-1}$ mg/g.min and $\beta = 1.07$ g/mg. For the intra-particle diffusion, the best fitted mechanism was obtained at 45 °C with the diffusion coefficient, k_{id} found to be 1.40×10^{-1} mg/gmin$^{1/2}$; the intercept of the q_t versus $t^{1/2}$ plot was -1.05×10^{-1} ($R^2 = 0.97$). The low value of the intercept suggests that the surface adsorption effect is minimal. Also, since the intercept of the plot did not pass through the origin, other surface phenomena are involved and the intra-particle diffusion is not the rate-limiting step [5]. In summary, the Elovich model best fitted at 25 °C,

Table 6 Kinetic constants at different temperatures

Models	25 °C	30 °C	35 °C	40 °C	45 °C	50 °C
PFO						
q_e	4.81	2.13	2.13	5.02	5.02	3.23
k_1 (g/mg/min)	6.16×10^{-2}	4.96×10^{-2}	6.68×10^{-2}	5.76×10^{-2}	10.48×10^{-2}	5.60×10^{-2}
R^2	0.953	0.977	0.879	0.740	0.677	0.877
PSO						
q_e	8.73	2.77	5.46	3.26	2.95	8.73
k_2 (g/mg/min)	2.46×10^{-4}	2.589×10^{-3}	7.21×10^{-4}	2.47×10^{-3}	2.81×10^{-3}	3.48×10^{-3}
R^2	0.150	0.646	0.589	0.897	0.945	0.915
Elovich						
α (mg/g min)	5.83×10^{-2}	5.06×10^{-2}	5.98×10^{-2}	6.33×10^{-2}	5.88×10^{-2}	5.16×10^{-2}
β (g/mg)	1.532	2.132	1.504	1.698	1.838	2.134
R^2	0.970	0.960	0.940	0.960	0.976	0.977
Intra-particle						
k_{id} (mg/g min$^{1/2}$)	1.97×10^{-1}	1.20×10^{-1}	1.62×10^{-1}	1.52×10^{-1}	1.40×10^{-1}	1.21×10^{-1}
I_i	-4.81×10^{-1}	-8.216×10^{-2}	-1.72×10^{-1}	-1.19×10^{-1}	-1.05×10^{-1}	-8.54×10^{-2}
R^2	0.947	0.941	0.935	0.970	0.971	0.967
Summary	Elovich	PFO	Elovich	Intra-particle	Elovich	Elovich

35 °C, 45 °C and 50 °C; PFO best fitted at 30 °C, while the intra-particle model best fitted at 40 °C. This is in line with similar work on adsorption carried out by [12].

Isotherms

The plots of the best fitted Langmuir, Temkin and Freundlich at 35 °C are shown in Figs. 12, 13, and 14. The isotherm constants and coefficient of determination for the ADS using Langmuir, Freundlich and Temkin Isotherms are shown in Table 7.

The analysis of the experimental data with the isotherms revealed the best adsorption occurred at 35 °C with a Langmuir constant, $K_L = -3.15 \times 10^{-4}$, ($R^2 = 0.93$) and the maximum adsorption capacity, $q_m = -5.98 \times 10^{-1}$ mg/g; a Freundlich constant, $K_F = 4.26 \times 10^{-11}$ g/mg ($R^2 = 0.98$) and adsorption intensity, $n = 0.28$ (this value of n less than 1 implied an unfavorable adsorption); and Temkin constant, $A = 1.42 \times 10^{-3}$ L/g, $B = 5.59$ and the Temkin constant related to heat of sorption, $b = 458.50$ J/mol ($R^2 = 0.97$), suggesting an endothermic process. The Freundlich isotherm fitted the experimental data significantly better than Temkin and Langmuir isotherms at this temperature.

Thermodynamic study

The plot of the Eyring equation is shown in Fig. 15, while the summary of the thermodynamic parameters for the adsorptive desulfurization is shown in Table 8.

The free energy change, ΔG°, was obtained at the different temperatures as shown in Table 8. The values of ΔG° increased as temperature increased. The positive ΔG° indicated non-spontaneous processes. The change in enthalpy ΔH° obtained was 96.03 kJ/mol. The positive ΔH° indicated an endothermic process. The change in entropy, ΔS°, obtained was − 23.87 J/mol·K. The negative value of ΔS° indicated decrease in randomness (or disorder) of the adsorbed species. Negative values of ΔS° (− 212.3 J/mol·K and − 0.11482 kJ/mol·K) were obtained in the adsorption of cyanide out of aqueous media by moderate density fiberboard saw dust (MDFSD) [6] and during the adsorption of methyl orange on coffee grounds activated carbon [18], respectively. Similar works on thermodynamic studies have been carried out by Olajire et al. [12] and Tanga et al. [19].

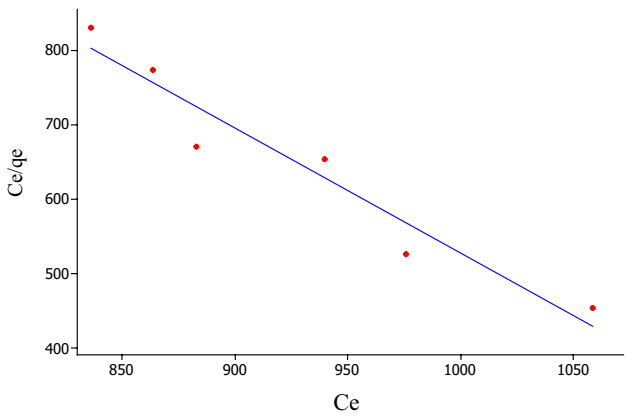

Fig. 12 Langmuir plot at 35 °C

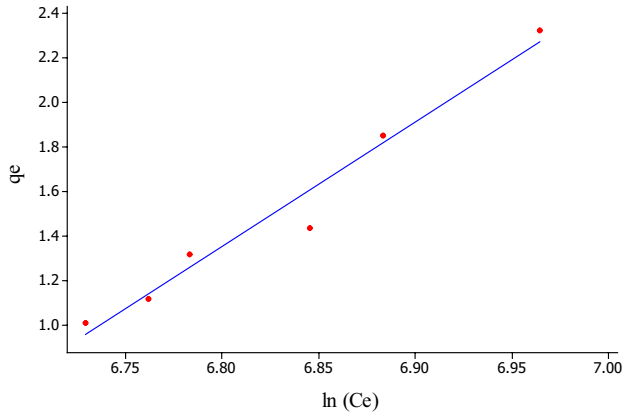

Fig. 13 Temkin plot at 35 °C

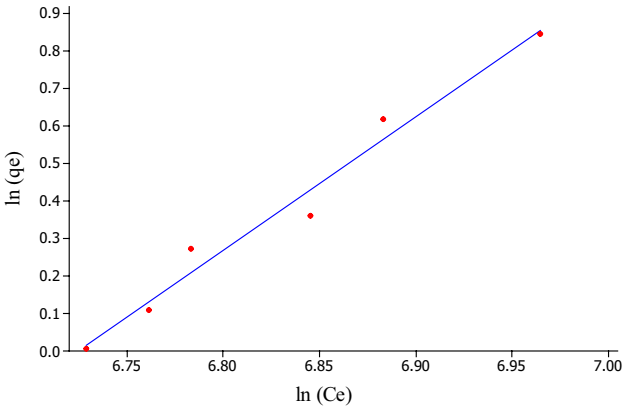

Fig. 14 Freundlich plot at 35 °C

Extent of adsorption

Figure 16 shows the plot of the extent of adsorption with time. The plot showed that 33% of desulfurization was achieved in 100 min.

Conclusion

The SEM, EDX and FTIR characterization of the ASS showed the ability of the sample to desulfurize diesel. The Elovich model best fitted the kinetic study suggesting that the ADS

Table 7 Langmuir, Freundlich and Temkin isotherm constants at different temperatures for the ADS

Isotherms at:	25 °C	30 °C	35 °C	40 °C	45 °C	50 °C
Langmuir						
K_L (g/mg)	6.21×10^{-4}	-3.15×10^{-4}	-7.60×10^{-4}	-7.13×10^{-4}	-7.91×10^{-4}	-8.35×10^{-4}
R^2	0.03	0.07	0.93	0.60	0.48	0.52
Freundlich						
K_F (mg/g)	1.47×10^{-2}	2.02×10^{-5}	4.26×10^{-11}	2.73×10^{-9}	1.01×10^{-11}	6.06×10^{-12}
n	1.66	0.63	0.28	0.34	0.29	0.26
R^2	0.08	0.46	0.98	0.8	0.67	0.70
Temkin						
A (L/g)	3.70×10^{-3}	1.81×10^{-3}	1.42×10^{-3}	1.53×10^{-3}	1.52×10^{-3}	1.49×10^{-3}
B	0.74	2.17	5.59	5.02	6.52	7.84
R^2	0.12	0.43	0.97	0.82	0.70	0.75

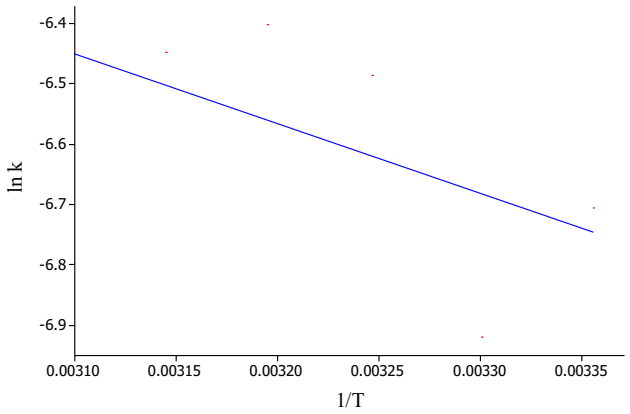

Fig. 15 Plot of the Eyring equation

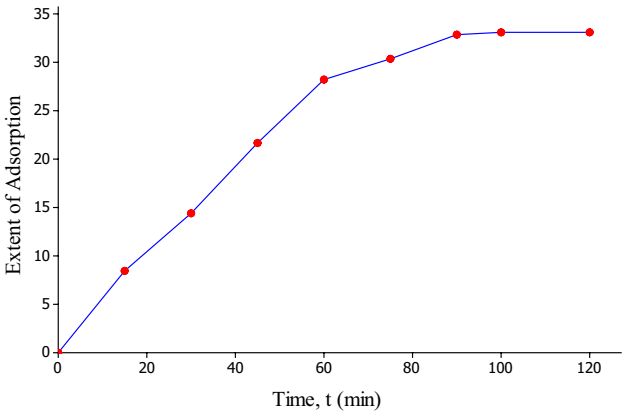

Fig. 16 Extent of adsorption time profile

Table 8 Thermodynamic parameters for the adsorptive desulfurization

Temperature (°C)	Thermodynamic parameters		
	ΔG° (kJ/mol)	ΔH° (kJ/mol)	ΔS° (J/mol.K)
25	16.72	96.03	−23.87
30	16.84		
35	16.95		
40	17.07		
45	17.19		
50	17.31		

of diesel with ASS followed this model. The study for the ADS revealed the best isotherms at 35 °C with Freundlich isotherm fitting the experimental data better than Temkin and Langmuir isotherms. The free energy change ΔG° values were found to be positive (indicating a non-spontaneous process) and increased as temperature increased. The positive ΔH° indicated an endothermic process, while the negative ΔS° indicated decrease in the randomness of the adsorbed species.

The adsorptive desulfurization of diesel was achieved using an adsorbent material developed from SS, activated with H_2O_2. 33% desulfurization was achieved in 100 min. The kinetics, equilibrium and thermodynamics parameters that suitably described the ADS of diesel at different temperatures were established, thereby providing necessary information for a scale-up process in addition to insight for mechanistic study.

Open Access This article is distributed under the terms of the Creative Commons Attribution 4.0 International License (http://creativecommons.org/licenses/by/4.0/), which permits unrestricted use, distribution, and reproduction in any medium, provided you give appropriate credit to the original author(s) and the source, provide a link to the Creative Commons license, and indicate if changes were made.

References

1. Ahmad W, Ahmad I, Ishaq M, Ihsan K (2014) Adsorptive desulfurization of kerosene and diesel oil by Zn impregnated montmorollonite clay. Arab J Chem 10:S3263–S3269
2. ASTM (1995) Annual book of standards. American Society for Testing and Materials, Philadelphia

3. Box GEP, Hunter WG, Hunter JS (1978) Statistics for experimenters: an introduction to design, data analysis and model building. Wiley, New York
4. Cheng BW, Ibrahim NA, Wan Yunus WMZ (2012) Optimization of tensile strength of poly(lactic acid)/grapheme nanocomposites using response surface methodology. Polym Plast Technol Eng 51(8):381–387
5. Hameed BH, Mahmoud DK, Ahmad AL (2008) Equilibrium modeling and kinetic studies on the adsorption of basic dye by a low-cost adsorbent: coconut (*Cocos Nucifera*) bunch waste. J Hazard Mater 158:65–72
6. Hisham JE, Elsousy KM, Hartany KA (2016) Kinetics, equilibrium and isotherm of the adsorption of cyanide by MDFSD. Arab J Chem 9:S198–S203
7. Izumi Y, Ohshiro T, Ogino H, Hine Y, Shimao M (1994) Selective desulfurization of dibenzothiophene by rhodococcus erythropolis D-1. Appl Environ Microbiol 60:223–226
8. Khodadadi A, Torabiangaji M, Talebizadeh Rafsanjani A, Yonesi A (2012) Adsorptive desulfurization of diesel fuel with nano copper oxide (CuO). Proceedings of the 4th International Conference on Nanostructures (ICNS4) 12–14 March, 2012, Kish Island, Iran
9. Kirimura K, Furuya T, Yoshitaka I, Kuniki K, Ken-ichi N (2003) Thermophilic biodesulfurization of hydrodeslfurized light gas oils by mycobacterium phlei, WU-FI. FEMS Microbiol Lett 221:137–142
10. Moreira AM, Brandão HL, Hackbarth FV, Maass D, Ulson de Souza AA, de Guelli U, Souza SMA (2017) Adsorptive desulfurization of heavy naphthenic oil: equilibrium and kinetic studies. Chem Eng Sci 172:23–31
11. Hadi NM, Rashid SA (2014) Deep desulfurization of diesel fuel by guard bed adsorption of activated carbon and locally prepared Cu-Y zeolite. J Eng 20(5):146
12. Olajire A, Abidemi JJ, Lateef A, Benson NU (2017) Adsorptive desulphurization of model oil by ag nanoparticles-modified activated carbon prepared from Brewer's spent grains. J Environ Chem Eng 5:147–159
13. Rashidi S, Nikou MRK, Anvaripour B (2015) Adsorptive desulfurization and denitrogenation of model fuel using HPW and NiO-HPW modified aluminosilicate mesostructures. Microporous Mesoporous Mater 211:134–141
14. Saleh TA, Danmaliki GI (2016) Adsorptive desulfurization of dibenzothiophenefrom fuels by rubber tyres-derived carbons: kinetics and isotherms evaluation. Process Saf Environ Protect 102:9–19
15. Selvavathi V, Meenakshisundaram A, Sairam B, Indra Neel P, Rajasekaran M, Viswanathan B (2008) Adsorptive desulphurization of diesel by modified carbons. 6th International Symposium on Fuels and Lubricants (ISFL-2008). New Delhi
16. Shah SS, Ahmad I, Ahmad W, Ishaq M, Gul K, Khan R, Khan H (2018) Study on adsorptive capability of acid activated charcoal for desulphurization of model and commercial fuel oil samples. J Environ Chem Eng 6:4037–4043
17. Sikarwar P, Arun Kumar UK, Gosu V, Subbaramaiah V (2018) Synergetic effect of cobalt-incorporated acid-activated GAC for adsorptive desulfurization of dbt under mild conditions. J Chem Eng Data 63(8):2975–2985
18. Rattanapan S, Srikram J, Kongsune P (2017) Adsorption of methyl orange on coffee grounds activated carbon. Energy Procedia 138:949–954
19. Tanga L, Yua J, Pang Y, Zenga G, Denga Y, Wanga J, Rena X, Yea S, Penga B, Fenga H (2018) Sustainable efficient adsorbent: alkali-acid modified magnetic Biochar derived from sewage sludge for aqueous organic contaminant removal. Chem Eng J 336:160–169
20. Thitiwan N, Sitthiphong P, Mali H (2013) Adsorptive desulfurization of dibenzothiophene by sewage-sludge derived activated carbon. Chem Eng J 228:236–271
21. Xiaoliang M, Lu S, Chunshan S (2003) Adsorptive desulfurization of diesel fuel over a metal sulfide-based adsorbent. Prepr Papers Am Chem Soc Div Fuel Chem 48(2):522
22. Reuters (2018) London. https://mobile.reuters.com/article/amp/idUSKCN1GP1HQ. Accessed 10 July 2018
23. Sahara Reporters (2018) New York. http://saharareporters.com/2018/03/15/nigeria-cut-sulphur-particle-fuel-july-says-nnpc. Accessed 10 July 2018